*Mineralogical Magazine, February 2008, Vol. 72(1), pp. 115–120*

# High-resolution imaging of biotite dissolution and measurement of activation energy

T. J. McMaster[1,*], M. M. Smits[2], S. J. Haward[1,4], J. R. Leake[2], S. Banwart[3] and K. V. Ragnarsdottir[4]

[1] H.H. Wills Physics Laboratory, University of Bristol, Bristol BS8 1TL, UK
[2] Department of Animal and Plant Sciences, Alfred Denny Building, University of Sheffield, Western Bank, Sheffield S10 2TN, UK
[3] Department of Civil and Structural Engineering, Kroto Research Institute, North Campus, University of Sheffield, Broad Lane, Sheffield S3 7HQ, UK
[4] Department of Earth Sciences, University of Bristol, Wills Memorial Building, Queen's Road, Bristol BS8 1RJ, UK

**ABSTRACT**

We have used a direct imaging technique, *in situ* atomic force microscopy (AFM) to observe the earliest stages of the dissolution of a biotite surface by oxalic acid at temperatures close to ambient conditions, using a specially designed AFM liquid cell and non-invasive intermittent contact mode of operation. From the nm-resolution data sets in x, y and z dimensions, we have measured dissolution rates and determined activation energies for the process as a function of temperature, via a mass-loss calculation. The value of $E_a$ obtained, 49±2 kJ mol$^{-1}$, appears to be too high to indicate a diffusion-controlled process and is more in line with expectations based on a process limited by the rate of ligand-induced metal cation detachment from the (001) surface. This is consistent with visual observations of the relative rates of etch-pit formation and growth, and accepted knowledge of the biotite crystal structure. Separate calculations based on planar area etch-pit growth, and measurements of etch-pit perimeters confirm this result, and also indicate substantially higher activation energy, up to 80 kJ mol$^{-1}$, when the edge pits are in an incipient stage.

## Introduction

The weathering of phyllosilicate minerals (e.g. mica) in soil is vital to the formation of clay minerals, e.g. vermiculite and smectite, and for the release of nutrients, such as K and Mg, into the soil solution for uptake by plants. It is postulated that the plants themselves, along with their associated symbiotic mycorrhizal fungi, may help to accelerate this process through the release of organic acid exudates. In this study we report the first real-time *in situ* observations of biotite (001) surface response to HCl and oxalic acid solutions using AFM to quantify dissolution rates and to characterize the development of etch-pitting. The relative effects of proton-promoted and ligand-promoted dissolution at the biotite (001) surface are investigated. The effects of temperature on the rates of oxalic acid dissolution of the biotite were determined using a novel system of temperature control, and an Arrhenius relationship for the dissolution of biotite is derived enabling the apparent activation energy of the reaction to be calculated. The results provide important new insights into the rates and processes of silicate weathering catalysed by oxalate, one of the most abundant low molecular-weight organic acids released into soil by fungi and associated microorganisms.

## Methods

### *Atomic force microscopy*

A Veeco Multimode AFM (NanoScope IIIA controller and Extender Module) was used for the experiments; for room temperature imaging a proprietary fluid cell was used, and at lower or higher temperatures a home-built modified liquid cell and flow system with temperature control was

* E-mail: t.mcmaster@bristol.ac.uk
DOI: 10.1180/minmag.2008.072.1.115

used. Contact Mode imaging was used to 'seed' the surface with a small number of etch pits and then Tapping Mode (Intermittent Contact) was used eliminating the frictional forces associated with Contact Mode. A 100 µl drop of 10 mM or 100 mM oxalic acid solution was placed with a syringe onto the freshly-cleaved biotite surface; the required temperature was reached and a time series of 1.25 µm × 1.25 µm AFM images acquired (periodically zooming out to 5 µm × 5 µm to check that the AFM scanning was not altering the rate of dissolution in the high-resolution image area).

### *Data analysis*

The AFM images were analysed using a 'bearing analysis' function to determine the percentage surface area occupied by etch pits; this percentage was then used to calculate the amount of dissolved biotite (in units of mol $m^{-2}$), using the known thickness of a biotite tetrahedral-octahedral-tetrahedral (TOT) layer ($T = 10^{-9}$ m), the density ($\rho$ = 3.09 $gcm^{-3}$) and biotite molecular weight ($M_w$ = 433.53 g $mol^{-1}$):

$$\text{biotite dissolved} = \text{fractional etch-pit coverage} \times xT \times \rho \times 10^6 / M_W \quad (1)$$

A plot of dissolution as a function of time was obtained from each set of images at different temperatures, and dissolution rates calculated, enabling an Arrhenius plot to be drawn according to the equation:

$$\ln(k) = \frac{-E_a}{RT} + \ln(A) \quad (2)$$

where $k$ = dissolution rate, $T$ = absolute temperature, $E_a$ = activation energy, A is the pre-exponential factor in the Arrhenius equation, and R is the ideal gas constant ($8.314 \times 10^{-3}$ kJ $mol^{-1}$ $K^{-1}$).

## Results

Figure 1 shows time sequences of tapping mode AFM images of biotite (001) surfaces in various acidic solutions at ambient temperature (~301 K). Sequences a and b start at $t$ = 0 minutes, defined as the time when the coverage of etch-pits, formed by acid applied to the surface, is equal to ~10% in each case, and is the first AFM image taken on switching from scanning to tapping mode. Subsequent images in the sequences are marked with the total passage of time since this first image was captured. Figure 1*a* shows such a sequence covering 1 h in time for biotite with 0.01 M oxalic acid (pH = 2). The surface degradation is seen to proceed by a combination of etch-pit formation and pit growth. Etch-pits are found to have a depth of 1 nm, consistent with

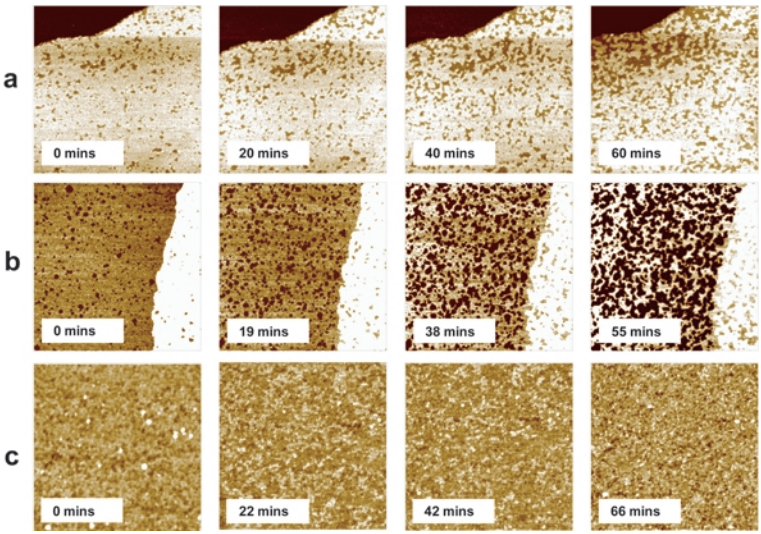


FIG. 1. Sequences of tapping-mode AFM images illustrating the dissolution of a biotite (001) surface in various acid conditions: (*a*) 0.01 M oxalic acid; (*b*) 0.1 M oxalic acid; (*c*) 0.1 M HCl. All images are of 1.25 µm × 1.25 µm, with a z range of 3 nm.

removal of a complete TOT layer. This correlates with the depth of etch-pits found on a muscovite (001) surface chemically weathered in the hyporheic zone of an Antarctic Dry Valley stream (Maurice *et al*., 2002). The loss of a complete TOT layer may result from leaching of the interlayer $K^+$, as suggested by e.g. Kalinowski and Schweda (1996). However, the apparent absence of remnants of undissolved tetrahedral or octahedral layers, which would probably be on the surface and affect the AFM image, is more suggestive of complete dissolution of the entire TOT layer.

For biotite in a 0.1 M solution of oxalic acid (pH ~1), Fig. 1*b*, the dissolution is seen to occur via similar processes of etch-pit formation and growth, although it clearly proceeds at a faster rate. For biotite in 0.1 M HCl, (Fig. 1*c*), the process of dissolution is visibly different and there is a general roughening of the biotite surface with the appearance of random etching. We suggest that the different morphologies arising from the application of HCl and oxalic acid occur due to the chelation of Al by the oxalate ligand, and this may have the effect of destabilizing the silica structure, leading to its more effective dissolution.

As the etch-pits expand, and more are formed, the dissolution rate gradually increases, probably due to increased surface area (Fig. 2). From the molecular weight and density of biotite it is possible to estimate the time required for dissolution of a complete TOT layer in each situation – in 0.01 M oxalic acid (pH 2) the time required is ~5 h/layer or alternatively 0.2 nm/h (equates to ~17 mm in 10,000 y, comparing favourably with the estimate of Malmström and Banwart (1997) of a rate of 1 mm in 10,000 y at pH 4).

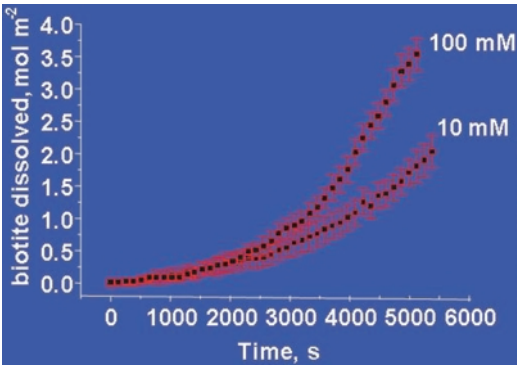


FIG. 2. Amount of dissolved biotite as a function of time in 0.1 M and 0.01 M oxalic acid solutions (derived from analysis of data in Fig. 1*a,b*).

The effect of temperature (283 K < $T$ < 308 K) on biotite dissolution is shown in the time-course sequence of images in Fig. 3*a–d*. As before, the first image ($t$ = 0) in each sequence represents an arbitrary starting point for the dissolution process where etch-pits cover ~10% of the surface in each case. It is very clear that the biotite surface dissolves more rapidly as the temperature is increased, but the processes of etch-pit formation appear similar at all temperatures. Analysis of the images in Fig. 3, along with the remainder of the images in each data set, provides the dissolution curves shown in Fig. 4*a*. The curves obtained at each experimental temperature all show qualitative similarities: slow dissolution associated with the initial formation of etch-pits (the formation of surface complexes) and a gradually increasing dissolution rate as etch-pits grow and access of acid to metals in TOT sites increases (detachment of the surface complexes). After some time the dissolution rate reaches a constant value, indicated in each case by the solid red line, which tends to start when etch-pits cover ~20% of the surface (this corresponds to $1.5 \times 10^{-6}$ mol m$^{-2}$ biotite dissolved). The analysis was terminated at ~50% etch-pit coverage ($4 \times 10^{-6}$ mol m$^{-2}$ dissolved biotite) due to the subsequent ligand promoted dissolution into the next underlying TOT layer. The gradients of the linear portions of the dissolution curves in Fig. 4*a*, indicated by the solid red lines, were taken to be the values of the dissolution rate, k, to be used for the determination of the activation energy, $E_a$, according to equation 2. The values of k are found to range from $4.3 \times 10^{-10}$ mol m$^{-2}$ s$^{-1}$ at 283 K up to $2.1 \times 10^{-9}$ mol m$^{-2}$ s$^{-1}$ at 308 K. These values lie at the lower end of the range of dissolution rates considered observable by *in situ* AFM (Dove and Platt, 1996). The Arrhenius plot resulting from the values of dissolution rate (Fig. 4*a*) is presented in Fig. 4*b*, and yields an apparent activation energy ($E_a$) for biotite dissolution in oxalic acid of 49±2 kJ mol$^{-1}$. This value is comparable to that of 60 ± 12 kJ mol$^{-1}$ determined by Jordan and Rammensee (1996) for brucite dissolution in acidic water using a similar method to that employed here. Our value also lies within the range of 30 kJ mol$^{-1}$ to 60 kJ mol$^{-1}$ found by White *et al.* (1999) for the release of various elements from granitoid rocks.

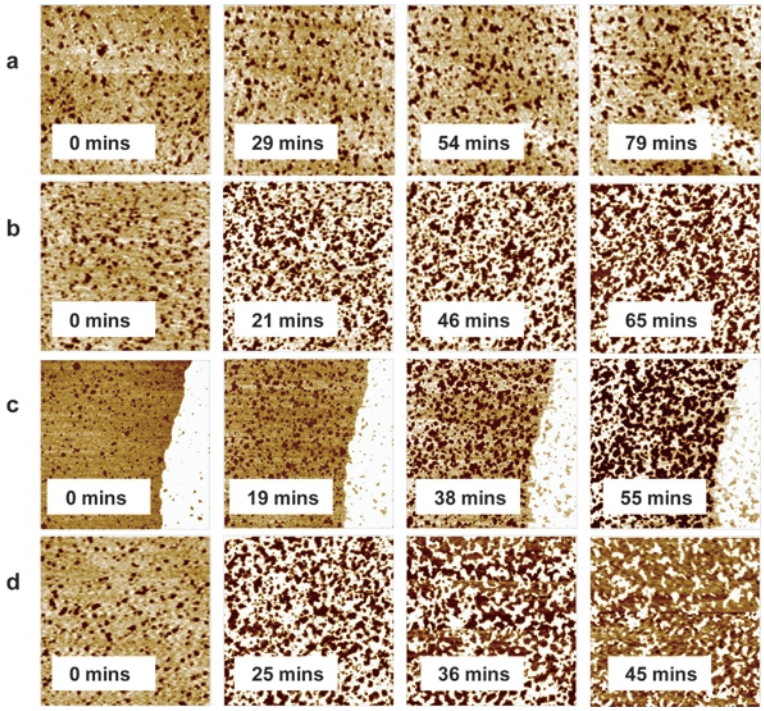


FIG. 3. Sequences of tapping-mode AFM images depicting the dissolution of a biotite (001) surface in 0.1 M oxalic acid at various temperatures: (*a*) 283 K; (*b*) 292 K; (*c*) 301 K; and (*d*) 308 K. All images are of area 1.25 μm × 1.25 μm, with a z range of 3 nm. The dissolution proceeds more rapidly as the temperature is increased.

Analysis of the planar growth of individual etch pits was also performed, resulting in a further supporting estimate of $E_a$. The average diameter of each etch pit was measured using image analysis software (Image Pro Plus), and a selection of 30 etch pits was followed over time for each temperature. A linear regression was applied to each etch pit, and average etch pit growth, at various temperatures, was calculated. Figure 5 shows the Arrhenius plot arising from these measurements and yields an apparent activation energy of $E_a$ = 51±9 kJ mol$^{-1}$, consistent with both of the previous estimates.

The correlation between the biotite dissolution rate and the density of step-edges present in the AFM scan area was also investigated. The

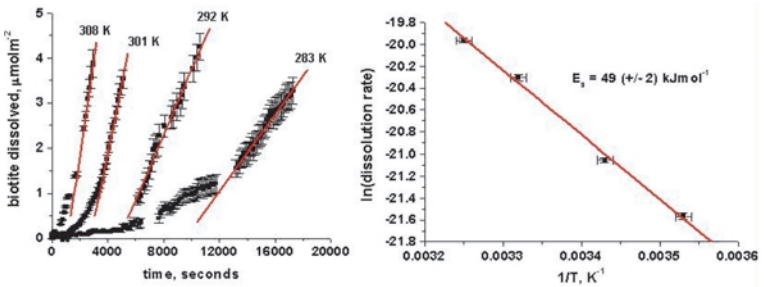


FIG. 4. (*a*) Amount of dissolved biotite as a function of time in 0.1 M oxalic acid at various temperatures. Solid red lines indicate the portions of the curves over which the dissolution is approximately linear with time; (*b*) Arrhenius plot for biotite dissolution in 0.1 M oxalic acid, showing the apparent activation energy, $E_a$ = 49±2 kJ mol$^{-1}$.

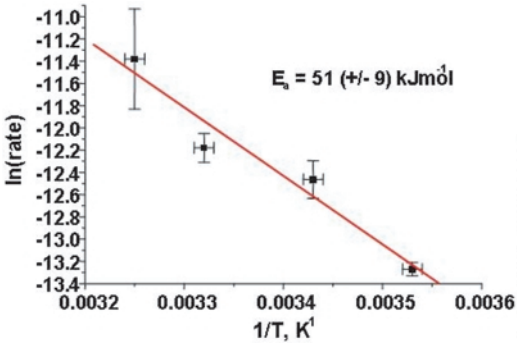


FIG. 5. Arrhenius plot calculated from measurement of planar growth of etch pits, yielding an apparent activation energy of $E_a$ = 51±9 kJ mol$^{-1}$, consistent with the analysis of Fig. 4.

dissolution rate was also calculated (Fig. 6*a*) by examining the difference in surface area loss between pairs of consecutive images and dividing by the time interval between the two images; the step density was determined by measuring the perimeter lengths of all the etch pits in each image, averaging, and dividing by the scan area. At 283 K and 301 K the straight lines-of-best-fit on Fig 6*a* pass very close through the origin, indicating that dissolution would not occur on the basal plane at these temperatures and would only occur at sheet edges. At 308 K, however, the line-of-best-fit passes significantly above the origin, indicating that at this temperature dissolution could proceed slowly even into a pristine (001) surface. Using lines of best fit from Fig. 6*a* provides a third way of calculating dissolution rate. At high step density the activation energy settles to a value of ~40 kJ mol$^{-1}$, slightly lower than our previous estimates; however, at low values of step density, the activation energy becomes extremely high. It is tempting to try to explain this in terms of a separation of two distinct processes involved in the dissolution: etch pit formation and etch pit growth.

## Conclusions

The value of $E_a$ ~50 kJmol$^{-1}$ for biotite dissolution in oxalic acid appears to be too high to indicate a diffusion-controlled process and is more in line with expectations based on a process limited by the rate of metal cation detachment from the (001) surface – consistent with our observations of relative rates of etch pit formation and growth. The emerging picture of the dissolution process of the (001) biotite surface in oxalic acid is of initial etch pit formation in the surface due to complexation of tetrahedral (probably primarily at $Al^{3+}$ sites) and octahedral ($Mg^{2+}$, $Fe^{2+}$) cations. This would expose the (001) crystal surface to attack, resulting in depletion of interlayer $K^+$ cations by displacement with $H^+$ and increasing the number of available sites for oxalate complexation with octahedral ions. This results in rapid growth of the etch pit, relative to the rate of etch pit formation in the pristine (001) surface. In the absence of oxalate (i.e. in HCl solution), the formation of discrete etch-pits is not observed, probably due to the lack of organic ligand to complex with $Al^{3+}$, and as a result, while interlayer and octahedral cations are still gradually detached, the silica skeleton remains relatively intact – resulting in a rough and perhaps amorphous surface structure.

## Acknowledgements

This work represents part of a NERC-funded Consortium grant on Mineral Weathering (NE/C521044/1) involving the Universities of Bristol,

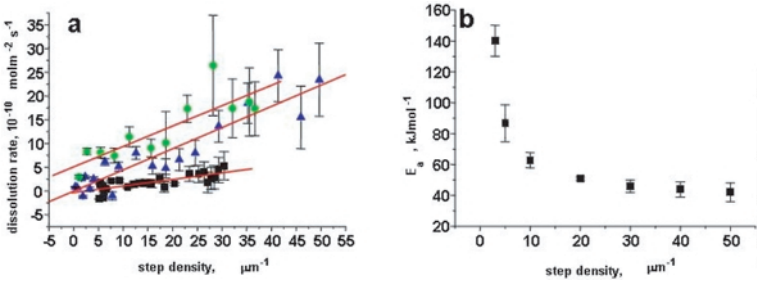


FIG. 6. (*a*) Dissolution rate calculated as a function of step density for biotite in 0.1 M oxalic acid at 283 K (squares), 301 K (triangles), 308 K (circles); (*b*) activation energy as a function of step density, derived from Fig. 6*a*.

Sheffield and Leeds http://www.wun.ac.uk/wsc/. This work is also linked to the EU-funded Marie Curie Training Network on Mineral Surface Science for Nanotechnology http://www.bris.ac.uk/mcest-mission/ (MEST-CT-2005-020828 MISSION).

## References

Dove, P.M. and Platt, F.M. (1996) Compatible real-time rates of mineral dissolution by Atomic Force Microscopy (AFM). *Chemical Geology*, **12**, 331–338.

Jordan, G. and Rammensee, W. (1996) Dissolution rates and activation energy for dissolution of brucite (001): A new method based on the microtopography of crystal surfaces. *Geochimical et Cosmochimica Acta*, **60**, 5055–5062.

Kalinowski, B.E. and Schweda, P. (1996) Kinetics of muscovite, phlogopite, and biotite dissolution and alteration at pH 1-4, room temperature. *Geochimica et Cosmochimica Acta*, **60**, 367–385.

Malmstrom, M. and Banwart S.A. (1997) Biotite dissolution at 25 degrees C: The pH dependence of dissolution rate and stoichiometry. *Geochimica et Cosmochimica Acta*, **61**, 2779–2799.

Maurice, P.A., McKnight, D.M., Leff, L., Fulghum, J.E. and Gooseff, M. (2002) Direct observations of aluminosilicate weathering in the hyporheic zone of an Antarctic Dry Valley stream. *Geochimica et Cosmochimica Acta*, **66**, 1335–1347.

White, A.F., Blum, A.E., Bullen, T.D., Vivit, D.V., Schulz, M. and Fitzpatrick, J. (1999) The effect of temperature on experimental and natural chemical weathering rates of granitoid rocks. *Geochimica et Cosmochimica Acta*, **63**, 3277–3291.